analytical chemistry

Feature

pubs.acs.org/ac

Photonic Lab-on-a-Chip: Integration of Optical Spectroscopy in Microfluidic Systems

The integration of micro-optical elements with microfluidics leads to the highly promising photonic lab-on-a-chip analytical systems (PhLoCs). In this work, we re-examine the main principles which are underneath the on-chip spectrophotometric detection, approaching the PhLoC concept to a nonexpert audience.

Isaac Rodríguez-Ruiz,[†,‡,§] Tobias N. Ackermann,[†,§] Xavier Muñoz-Berbel,[†] and Andreu Llobera*[,†]

[†]Institut de Microelectrònica de Barcelona−CNM/CSIC Campus UAB, 08193 Cerdanyola del Vallès, Barcelona, Spain

[‡]CEA, DEN, DTEC, SGCS, F-30207 Bagnols-sur-Cèze, France

Supporting Information

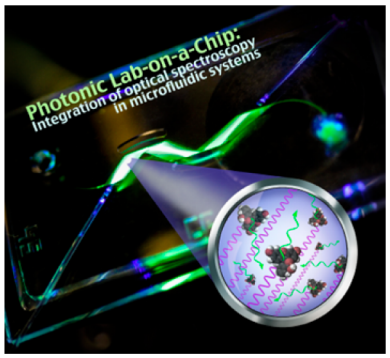

With the aim to miniaturize and integrate most of the required steps of an analytical assay, lab-on-a-chip (LoC) technology has gained significant weight in the last 2 decades. In this context, miniaturization allows not only a decrease of the required analysis time, sample volume, and reagent consumption but also results in an enhancement of the sensitivity and the possibility to parallelize the analysis without dramatically increasing both the complexity and the system footprint. As a result, from the early micro total analysis system (μTAS) concept,[1] nowadays it is possible to find in the literature a myriad of extremely sophisticated LoC for applications such as drug discovery and development,[2] genomics,[3] clinical diagnosis,[4] or cellomics.[5] In most of these examples, a superior performance as compared to bulk analytical setups in terms of sensitivity to a specific analyte is obtained.

However, most of the LoCs still rely on external and complex instrumentation for analyte detection and quantification. As a result, they still fail to be more widely established alongside standardized laboratory protocols and techniques and, more importantly, in real applications outside controlled laboratory environment. The integration of transducers able to transform a biological/chemical reaction into a quantifiable signal will represent a turning point of the LoC paradigm. Steps toward this issue have been taken and different transduction mechanisms have already been integrated in a LoC, such as electrochemical,[6] magnetic,[7] or optics/photonics.[8] Among them, optical transducers have demonstrated to be one of the most sensitive and selective analytical detection methods,[9] while providing the unmatched property of prevailing sample sterility due to its noncontact measurement principle.

Light manipulation and confinement in liquid materials, and specially in microfluidic environments, has generally been called optofluidics.[10] In one branch of optofluidics, fluids play an active, key role in handling, and directing the propagation of light in the microsystem (however, this is a step further in complexity). A major advantage here is the atom-sized roughness between two immiscible fluids with different refractive index (RI), resulting in optically flat surfaces. Not surprisingly, this concept has been exploited in liquid−liquid waveguides[12] and in optofluidic routers.[13]

Alternatively, the synergistic combination of photonic integrated circuits (PICs) with LoC gives rise to the photonic lab-on-a-chip (PhLoC) concept,[11] where the advantages of both research fields are merged. Here, the main function of microfluidics is the manipulation and transport of the analytes, while the PICs transduce the (bio)chemical signal arising from the analytes in situ to a quantifiable signal.

In this work we aim to provide an introduction to the integration of optical spectroscopy with LoC by means of fundamental optical elements, i.e., microlenses and mirrors. We describe the nuts and bolts of the conception of such PhLoC systems based on two main keystones: (i) the selection of the appropriate detection mechanism, i.e., colorimetry, fluorimetry, and/or dispersion/scattering, and (ii) the design of the PhLoC, considering both the optical properties of the materials and the geometry of the optical elements. Finally, the application of this paradigm is demonstrated through some examples showing different and low cost approaches to solve real analytical problems.

BASIC PRINCIPLES: SPECTROPHOTOMETRIC MEASUREMENTS ON CHIP

Within the previously mentioned spectrophotometric techniques, both colorimetry and scattering assays can be measured longitudinally through the bulk of the sample. The propagation through the sample results in an attenuation of the light, which

Published: May 6, 2016

DOI: 10.1021/acs.analchem.6b00377
Anal. Chem. 2016, 88, 6630−6637

is proportional to the optical path length l (cm^{-1}) and the analyte concentration c (M), and is described by the Beer–Lambert law:[14]

$$A(\lambda) = -\log_{10}\left(\frac{I}{I_o}\right) = \varepsilon(\lambda)cl \quad (1)$$

where I_o is the reference intensity measured through l in absence of analyte (e.g., only solvent), I is the intensity measured through the same optical path in presence of analyte, and ε is the molar attenuation coefficient of the analyte (M^{-1} cm^{-1}), which varies as a function of the wavelength. Note that in most cases the attenuation of the sample (extendedly called absorbance A with absorbance units A.U.) is due to absorption as well as scattering. Scattering events do however not add linearly to extinction. Depending on the scattering anisotropy (g, dimensionless) of the analyte, a portion of light is scattered in the forward direction ($g = 1$ implies purely forward, $g = 0$ backward scattering) and still detected in the longitudinal direction.

It should also be mentioned that not only the analyte itself contributes to attenuation of the incident beam. Reflections at interfaces (depending on the contrast of refractive index at the interface) as well as the proper solvent may also cause attenuation. It is thus crucial for the accuracy of the measurement that I_o (which corresponds to 100% transmittance) is measured with the same optical system and same interface conditions as used to measure I.

Experimentally, it is accepted that eq 1 presents a linear behavior for absorbance values within 0 and 1 A.U. The deviation from the linearity postulated by the Beer–Lambert law is commonly observed for high analyte concentrations for a fixed l value, e.g., due to a change in refractive index of the solution or aggregate formation, which is not considered in the Beer–Lambert law derivation. The sensitivity of such measurements is given by the slope in the linear range. It is reasonable to consider that the shorter the optical path, the lower the sensitivity, though the contrary (i.e., the longer the optical path, the higher sensitivity) does not apply *ad infinitum*, as there are other factors working against. First, it must be considered that light sources are inherently divergent and, unless proper 3D optical elements are included in the microsystem, the optical losses increase with the optical path length. As a consequence, the signal-to-noise ratio (SNR) quickly decreases for large optical paths. Additionally, we also need to satisfy the compactness constraint required for LoC applications.

In contrast to colorimetry and scattering assays as described above, fluorimetry does not rely on the quantification of attenuation. Fluorescence is the transition from an absorption induced excited electronic state to a state with a lower energy by emission of a photon. As such it is proportional to absorption, but the emission occurs spontaneously in 4π steradians at a ratio of emitted versus absorbed photons called the quantum yield Φ. This homogeneous light emission allows multiplexing excitation and emission wavelengths when the detector is positioned 90° from the light source. In that way the fluorescence emission intensity can be decoupled from the excitation radiation, thus improving the SNR for the detection of light emitted by the analyte. It should however be kept in mind here that only a fraction of light emitted with the appropriate solid angle can be detected, unless integrating spheres are used. Under the assumption that attenuation is here solely due to absorption, the fluorescence intensity measured at wavelength λ_F can then be written as

$$I_F \propto k\Phi(1 - (10^{-A})) = k\Phi I_0(1 - (10^{-\varepsilon cl})) \quad (2)$$

where the proportionality factor k depends on several parameters, in particular on the optical configuration for observation (i.e., the solid angle through which the instrument collects fluorescence) and ε refers strictly to absorption. For low analyte concentrations (and accordingly low absorption along the optical path), eq 2 can be approximated to[15]

$$F = kI_0\Phi(\varepsilon cl) \quad (3)$$

Consequently, in order to perform classical spectrophotometric analyses on-chip with enhanced sensitivity, it is important to attune the PhLoC design to the specific application and to optimize crucial parameters. In particular, the use of micro-optic elements for light collimation or focusing can be very useful for boosting light coupling/decoupling efficiency and accuracy as well as optimizing light-sample interaction in optofluidic systems.

Micro-Optics Design and Fabrication. The design of micro-optic elements still complies with the basic optics laws as long as the diffraction limit is not reached. As such, the following assumptions must be considered.

From a practical point of view, one of the simplest ways to couple light to/from a PhLoC is by way of pigtailed fiber optics, as these represent a standardized link to a wide range of light sources as well as photodetectors and photospectrometers. Thus, if the micro-optic elements are designed in accordance to the fiber optics parameters (numerical aperture and core diameter mainly), they can be readily included in the PhLoC as a basic element independent of the particular application.

Concerning the concrete optical design it should be mentioned that a light beam is bent at an interface between two materials according to the well-known Snell's law,[16]

$$n_1 \sin(\theta_1) = n_2 \sin(\theta_2) \quad (4)$$

where n_1 and n_2 are the respective refractive indices of the adjacent materials and θ_1 and θ_2 are, respectively, the incident angle in the first material (with respect to the surface normal) and the new angle after passing the interface.

Equation 4 provides the basic tool to understand beam propagation at the interface between two materials by knowing the incidence angle and the involved refractive indices. Another implication of eq 4 is that there exists a critical angle of incidence

$$\theta_c = \sin^{-1}\left(\frac{n_1}{n_2}\right) \quad (5)$$

above which light is totally internally reflected (TIR condition). Accordingly, the contrast in refractive index at an interphase between adjacent materials can also be used to define mirrors, which act upon all rays fulfilling this condition.

A second well-known formula is the so-called lensmaker's equation[16]

$$\frac{1}{f} = (n_1 - 1)\left[\frac{1}{R_1} - \frac{1}{R_2} + \frac{(n_1 - 1)d}{R_1R_2}\right] \quad (6)$$

where f is the focal length, R_1 and R_2 are the radius of curvature, and d is the thickness of the lens (which can be considered zero for thin lenses). Thus, by carefully combining curved interfaces

DOI: 10.1021/acs.analchem.6b00377
Anal. Chem. 2016, 88, 6630–6637

(as shown in Figure 1a) with known refractive indices, light shape, and propagation can be modified so as to match with the specific requirements of a given PhLoC application. It is important here to say that what is required for managing the light flow is an interface between two materials with different refractive indices. The most common (and sometimes overlooked) material is air, which can indeed be used as an active material for defining any kind of micro-optical element.

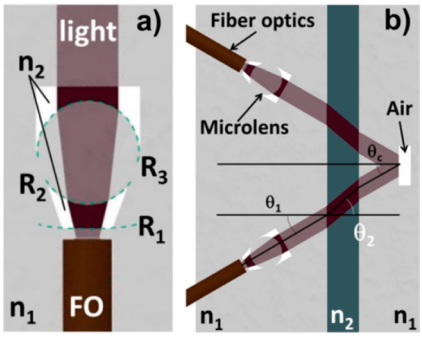

Figure 1. Schematic representations of (a) the conception of a collimating set of lenses with curvature radii $R_{\{1-3\}}$ optimized for the use with fiber optics of a defined numerical aperture and (b) the interaction of different micro-optic elements to enhance light−sample interaction: A first set of microlenses collimates the incoming beam, which then travels across the microchannel filled with analyte, is reflected back across the channel and finally focused on the output fiber optics by the second inversely operated set of microlenses. Figure adapted from ref 17 and reproduced with permission of Nature Protocols. Copyright 2011 Nature Publishing Group.

Optofluidic System Design. Figure 1b schematically shows one example of how these optical phenomena can be employed in a PhLoC, combining two sets of collimating microlenses, light-sample interaction, and a flat air mirror to double the optical path through the sample. Initially, the fiber optics is inserted in so-called self-alignment channels, which allow clamping the fiber optics at the required specific distance from the lens, typically the focal length, and perfectly aligned with the optical axis. Light arising from a pigtailed fiber optics is collimated by a first set of focusing cylindrical lenses (Figure 1a; the figure can be found in the Supporting Information). Specifically, the imprinted air structures of the microlenses comprise curved surfaces, whose curvature radii are chosen based on the refractive index contrast between air and the construction material. Thus, a major part of the incoming light can be directed along the intended axis and interact with the analyte in the microfluidic channel. The refraction of the beam at the interphase between construction material (n_1) and the analyte solution (n_2) according to eq 2 is also to be considered in the design for correct relative positioning. After crossing the channel, the collimated beam strikes a flat air pocket (air mirror) with an incident angle above θ_c and is consequently reflected back across the channel and focused onto the tip of an output fiber optics via a set of inversely operated microlenses. Given this working principle, it is shown that a set of geometric considerations such as radii of curvature and angles of incidence, based on the construction material at hand, allows one to construct micro-optical elements for precise and efficient light handling, suitable for the integration in PhLoCs. Another important issue is that the integration of such micro-optical elements does not increase the technological complexity, since they can be implemented jointly with the microfluidics mask.

Fabrication. A fabrication technique especially suited to integrate such micro-optical elements in microfluidic systems is soft-lithography.[17] The technique is well-established in the domain of μTAS and is based on the direct transfer of planar structures with features in the micro- and nanoscale from prepatterned molds or stamps, so-called masters, into soft elastomeric materials with high transparency at UV−vis wavelengths. One of the most widely used materials fulfilling these requirements is polydimethylsiloxane (PDMS), a silicon-based organic polymer which is optically clear, cheap, and nontoxic. The replicas, made with PDMS or any other material, feature the negative of the patterns contained in the masters as imprints (air gaps) with well-defined geometry. In this way, PhLoC systems can be monolithically imprinted in a single step, assuring a perfect alignment of micro-optic and microfluidic elements by design. Moreover, the resulting alternation between air and construction material in the optical path provides with the required refractive index contrast and therefore efficient light beam modulation by the interphases.

APPLYING AND DEVELOPING THE BASIC CONCEPTS

Single and Multiple Internal Reflection. From eq 1 it becomes clear that PhLoCs working in absorbance should ideally have the longest possible optical path, so as to enhance its sensitivity. It must be kept in mind, however, that the microlenses fabricated with soft lithography are not spherical but cylindrical. As such, they do not have a focal point but rather a focal plane (light sheet). In other words, the beam broadening in the vertical direction is not corrected, thus decreasing the SNR. Still, with the help of the air mirrors it is possible to lengthen the optical path in a PhLoC without causing an important increase of the footprint. In that sense, the simplest configuration is based on the so-called single internal reflection (SIR) systems,[18] which can be seen in Figure 2a. Light is coupled by means of a biconvex microlens to a hollow Abbe prism. With the help of a flat air mirror, light bounces with a 60° angle toward the second biconvex microlenses and is finally collected with the output fiber optics. Such SIR PhLoCs have been applied for measurements of fluorescein[19] and methylorange,[20] for the detection of heavy metal ions[21] or as an element of an optical-electrochemical tongue for the quality control of wine.[22]

Furthermore, with the adequate enzymatic functionalization, the prisms have been transformed into biocatalytic sensing reactors where enzyme activity has been measured.[23] An overview of the different applications, each PhLoC configuration and their respective limit of detection (LoD) (using a k value of 3, ensuring a confidence level of 99.87%)[24] can be found in Table 1, together with other PhLoC applications and configurations. Sensitivity can be further enhanced by increasing the optical path, but at a cost of increasing the SIR system size. An alternative is to shift from single to multiple reflections. Air mirrors can be defined at both sides of a given microfluidic system and then, by means of TIR, make light follow a zigzag path. In addition, the shape of the air mirrors can be arbitrarily defined: in that sense, in Figure 2b, focusing air mirrors allow one to have focal planes inside the microfluidic system. Note that the use of focusing elements implies the necessity to adapt the channel length to the focal length. These kind of PhLoCs, called multiple internal reflection (MIR)

DOI: 10.1021/acs.analchem.6b00377
Anal. Chem. 2016, 88, 6630−6637

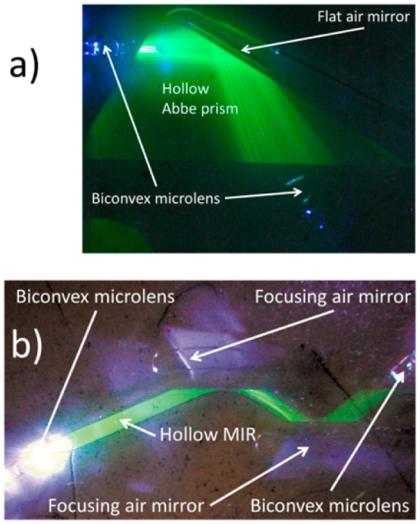

Figure 2. (a) SIR structure filled with buffer solution + 50 μM of fluorescein, where light reflection can be seen at the air mirror; (b) MIR structure filled with buffer solution + 10 μM of fluorescein, showing the zigzag path of the light inside the sensing region. Figures published in refs 11 and 18 and reproduced by permission of The Royal Society of Chemistry. Copyright 2007 and 2008, respectively.

systems, have demonstrated to have LoDs between 110 nM and 41 nM for fluorescein.[11] The potential of the MIR configuration is confirmed by the large number of applications and configuration where it has been used, e.g., in combination with electrochemical sensors (defining the Dual LoC) for L-lactate measurements[25] or for the classification of white grape juices with a multisensor (tongue) approach.[26] Additionally, they have been used as reactors for screening cell cultures, working in either scattering or scattering + absorption regimes, both with LoDs close to 50 cells using monocytes and being able to distinguish between labeled (dead) and nonlabeled (alive) cells.[17,27] A further step toward integration has been done by monolithically integrating a xerogel-based solid-state light emitter (SSLE) with a biofunctionalized MIR for detecting biocatalytic activity at very low substrate concentrations in the micromolar range.[28] A list of the different analytes measured with MIR structures can be found in Table 1.

Multiple Measurement Parallelization. Once a first degree of PhLoC complexity by the integration of microlenses for light beam collimation was achieved and taking advantage of MIR to elongate the interrogated optical path through the samples, a step forward in complexity is presented in the Multiple Path Photonic Lab-on-a-Chip (MPhIL).[29] This system, yet based on the same principles, allows the parallelization of multiple measurements within the same sample. MPhIL consists of a single serpentine channel describing 6 interconnected and different optical paths with lengths l varying from 0.05 to 1 cm (Figure 3a). In the case here described, optical interrogation channels (Figure 3a-1) comprise similar self-alignment elements and 2D microlenses to correct the beam broadening (Figure 1a-2). Air mirrors (Figure 3a-3) are located at both sides of the optical path with a 2-fold function: On the one hand, they form a waveguide-like structure by confining the light in the region where the microfluidics (and the analyte) is located, as it can be observed in the ray tracing simulation shown in Figure 3a-4. On the other hand, background noise and crosstalk is minimized, since such air mirrors allow one to block part of the light arising from either adjacent interrogation channels or from any other external source.

The MPhIL is based on multiple parallel absorbance measurements at constant concentration, performed on a single sample, while varying the optical path length. The so-

Table 1. Analytes, Configuration and LoD of the Different PhLoC Configurations Found in the Literature

Analyte	Configuration[a]	Type of measurement	LoD [μM]	Optical path [μm]	ref
Fluorescein	SIR	Fluorescence/absorbance	6	2387	19
Fluorescein	SIR	Fluorescence/absorbance	1.3−5.6	1790−3581	20
Fluorescein	SIR	Fluorescence/absorbance	1.03−1.08	2766, 3581	18
Methylorange	SIR	Absorbance	0.68−2.5	1790−3581	20
Methylorange	SIR	Absorbance	0.39	2766, 3581	18
pH	SIR	Absorbance	0.09−0.51	1790−3581	20
Wine	SIR (hybrid tongue)	Absorbance	-	3581	22
H_2O_2	SIR+enzymatic functionalization (HRP)	Absorbance	0.12	3581	23
Hg^{2+}/Pb^{2+}	SIR+ specific ligand	Absorbance	2.59/4.19	3581	21
Fluorescein	MIR	Fluorescence/absorbance	0.04−0.1	6357−14264	13
Monocytes	MIR	Absorbance/scattering	50 cells	8336	26, 17
L-Lactate	MIR+electrode	Absorbance	5	6357	24
Wine	MIR (tongue)	Absorbance	-	6357	25
Quinolone yellow/ H_2O_2	MIR+SSLE	Absorbance	0.6/0.7	6357	27
Proteins	Multiple path LALC	UV-Absorbance	1.28/8.5	500−10000	29
H_2O_2	[b]LALC+enzymatic functionalization (HRP)	Absorbance	4.53	1000	25
Organic solvents	LALC	Absorbance	-	3000	2b
pH/Bacteria	LALC	Absorbance (180°)/ Fluorescence (90°)	0.32- 4.60 × 10^6 cells	4200−5000	33
Crystal violet	MOPS	Absorbance (180°)/ Fuorescence (90°)	0.34 -	10500	36

[a]All the PhLoC configurations presented are fabricated in PDMS (n = 1.41 at λ = 633 nm), except for ref 2b, fabricated in SU-8 (n = 1.58 at λ = 633 nm). [b]LALC, micro-Lens-Assisted Light Collimation. Direct measurements performed with light input/output configured at 180°.

DOI: 10.1021/acs.analchem.6b00377
Anal. Chem. 2016, 88, 6630−6637

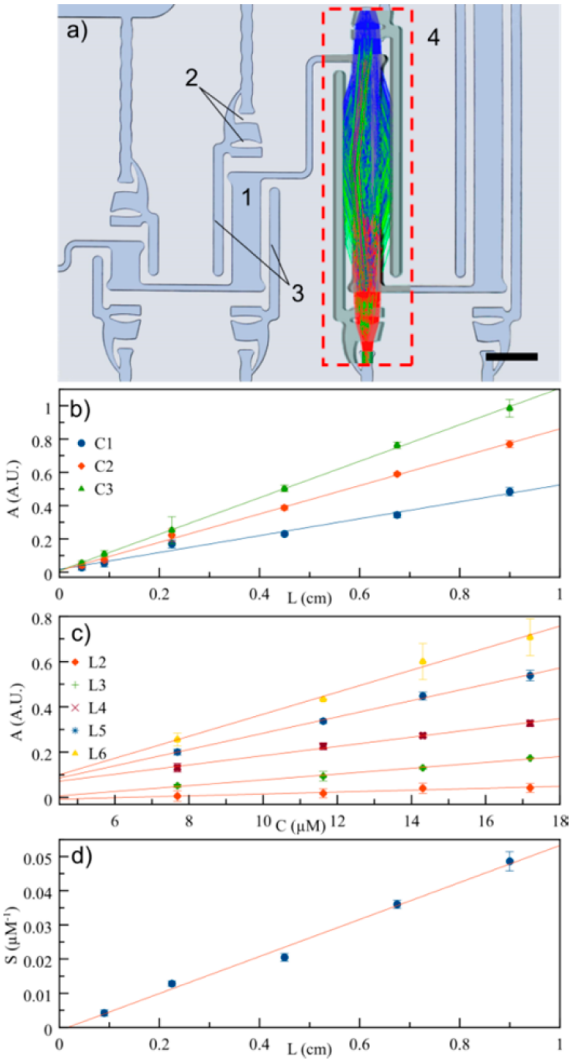

Figure 3. (a) Detail of a fabricated MPHIL. 2D microlenses and fiber optics channels can be seen at the ends of each optical path. (1) 2D microlenses; (2) air mirrors to prevent cross talking; (3) interrogation channel. Scale bar = 1 mm; (4) overlapped screenshot of a ray tracing simulation across one MPHIL OP, illustrating the performance of the included micro-optical elements (air mirrors and microlenses). (b) Plot of the absorbance measurements performed in the MPHIL as a function of different glucose isomerase protein concentrations for each MPHIL optical path. (c) Plot of the analytical sensitivity, S, as a function of optical path length. From the linear regression analysis of this plot, it is possible to calculate a limit path length of $L = (9.42 \pm 0.29) \times 10^{-2}$ cm. (d) Plots of the absorbance measurements performed with 3 different concentrations for dihydropyrimidinase from *S. meliloti* CECT41 protein, as a function of the optical path length (L): $C_1 = (8.37 \pm 0.03)$ μM, $C_2 = (14.03 \pm 0.09)$ μM, $C_3 = (18.0 \pm 0.1)$ μM. Data adapted from ref 29 and reproduced by permission of The Royal Society of Chemistry. Copyright 2015.

called multiple path PhLoC configuration presents a series of advantages: it allows an increase in the linearity range relating concentration and absorbance in accordance to the Beer–Lambert law, as the measurements performed at shorter l values are transduced in a decrease of the absorbance signal (1). Additionally, analyte concentration or molar absorptivity can be obtained with a single injection step, as opposite to the standard calibration protocol, which requires a series of measurements at different concentrations. Figure 3b shows absorbance experiments at $\lambda = 280$ nm, performed at 3 different concentrations for dihydropyrimidinase from *Sinorhizobium meliloti* CECT41 protein as a function of l, displaying the linear relation between both values, in agreement with eq 1. Protein concentrations were selected to present an absorbance below 1 A.U. (at $\lambda = 280$ nm) in the largest optical path of the MPhIL, allowing the parallel use of the 6 different optical paths for the measurements. R^2 coefficients calculated from the least-squares linear fitting of the data showed a good correlation degree ($R^2 > 0.98$) for all the measured concentrations.[29]

Aside, the LoD for each optical path was also calculated. Using the above-mentioned analytical definition of LoD,[24] it is also possible to determine a limit value for the optical path lengths, allowing this to dynamically determine the optimal l values as a function of the analyte of interest. Calculations for this purpose were performed using another protein, glucose isomerase, as a model for the determination. Absorbance measurements as a function of different protein concentrations for each optical path are plotted in Figure 3c with their respective fittings, also displaying a good correlation. LoD values between (1.28 ± 0.04) μM and (8.5 ± 1.8) μM, respectively, for the largest and shortest l are obtained for the model protein. Extracting the analytical sensitivity (S) from this plot (the slope of each linear fitting) and representing it as a function of the optical path (Figure 3d) we can determine a limit path length by means of a another linear fitting analysis, obtaining a value of $L = (9.9 \pm 0.5) \times 10^{-2}$ cm. This limit path length value will correspond to the minimum l which would provide a measurable absorbance signal for the range of the studied analyte concentrations.

It is worth noting that the MPhIL can also be implemented and used as a multispectral detection component in more complex lab-on-a-chip systems, where the different multiple paths would permit both detection and quantification of the target analytes. Besides, the system is able to operate in the continuous flow regime, making it a good candidate to be used as a detection system for continuous sensing applications.

TOWARD ADVANCED SYSTEM INTEGRATION AND CONFIGURATION

Biophotonic Lab-on-a-Chip. One of the areas where microfluidics advantages are more efficiently exploited is in cell culturing.[30] *In vitro* cell cultures are currently the mainstay of experimental cell biological research for being the simplest model that sufficiently represents human biology and disease.[31] Microfluidics provides systems for cell culturing that expand the capacity to, spatially and temporally, control local microenvironments, while minimizing potentially error-prone laboratory manipulations.[32]

This motivation is the base of the biophotonic lab-on-a-chip (bioPhLoC) architecture that is described below.[33] This bioPhLoC allows a strict control of environmental conditions during cell proliferation and the simultaneous (and independent) analysis of cells and supernatant during the assay. To this end, the bioPhLoC is designed with two independent and fluidically connected (Figure 4a) chambers: the incubation and the monitoring chambers. The incubation chamber monolithically integrates 3 μm high microchannels (Figure 4b) which act as a size-exclusion microfilter. That is, small particles (<3 μm), such as *Escherichia coli* bacteria, can cross the filter, whereas big particles (e.g., yeasts or mammalian cells) will be retained in the incubation chamber. In the case of mammalian cell cultures this configuration is advantageous for several reasons. First, all cells

DOI: 10.1021/acs.analchem.6b00377
Anal. Chem. 2016, 88, 6630–6637

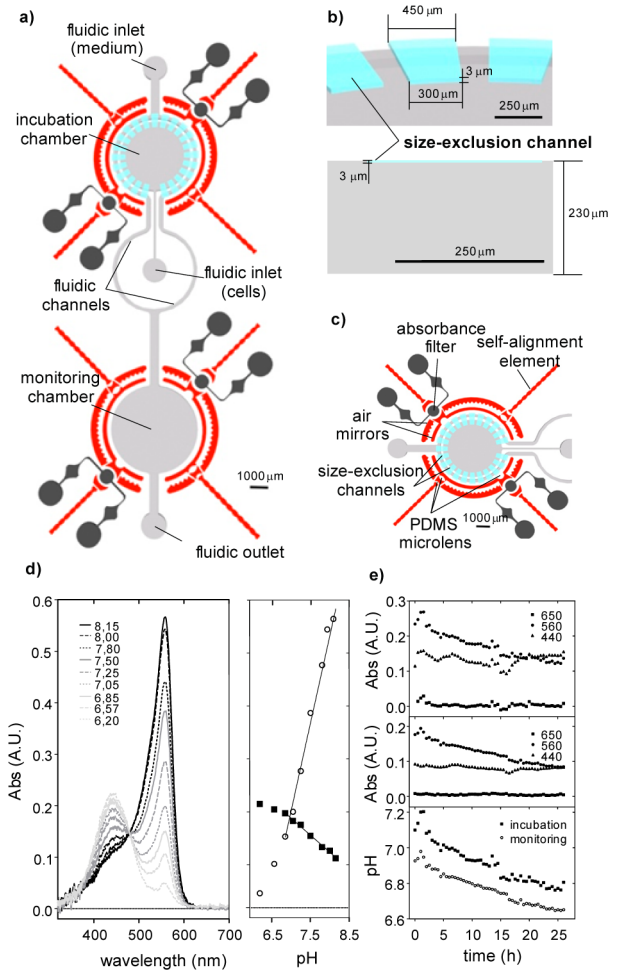

Figure 4. (a) Drawing of the bioPhLoC indicating the fluidic elements integrated on its structure (in gray in the figure); (b) 3D representation and cross section of the size-exclusion microchannels of the filter (in blue in the figure) integrated in the incubation chamber; (c) detail of the optical elements integrated in each chamber of the bioPhLoC; (d) absorbance spectra at wavelengths ranging from 350 to 900 nm for DMEM solutions at pH ranging from 8.15 to 6.20. The variation of the absorbance at wavelengths of 560 and 440 nm with the pH is also represented (Error bars show the standard deviation of three repetitive measurements.); (e) absorbance variation with time during seeding, trapping, and rinsing stages at wavelengths of 440, 560, and 650 nm, in the incubation (top) and monitoring chambers (medium). In the bottom plot, pH variation (from 560 nm wavelength) with time during seeding, trapping, and rinsing stages in the incubation and monitoring chambers. Figures published in ref 33 and reproduced by permission of The Royal Society of Chemistry. Copyright 2013.

inoculated will be retained and concentrated in the incubation chamber, which minimizes the number of cells lost during the experiment. Additionally, the presence of the filter restricts cell proliferation to the incubation chamber, improving the control of the culture and allowing the separated monitoring of cells and supernatant, without any additional separation process.

For cells and supernatant analysis, both chambers contain micro-optical elements for optical transduction analogous to the ones previously described, namely, self-alignment elements, collimation lenses, air mirrors for light confinement, and also include absorbance filters whose function will be described below (Figure 4c). The bioPhLoC is very versatile and allows colorimetric, dispersion, and/or fluorescence analysis of the cells in the incubation chamber or the supernatant in the monitoring chamber. This can be achieved by just modifying the number and/or position of the fiber optics inserted in the system. That is, with a 180° configuration (fiber optics facing one another), it is possible to perform absorbance or scattering measurements, whereas at 90° it is possible to carry out fluorescence and/or wide angle dispersion analysis. Absorbance filters can be integrated in the bioPhLoC architecture by using sol−gel technology[34] and may improve fluorescence measurements by partially removing the excitation light from the collected signal, therefore increasing the SNR. The measurement of model molecules/particles (i.e., methylorange, absorption at 470 nm, and *Escherichia coli*, dispersion at 600 nm) validates the performance of the micro-optical elements integrated therein for colorimetric and/or dispersion analysis.

Finally, the bioPhLoC is applied to the simultaneous detection of pH changes in the cells and the supernatant using vascular smooth muscle cells (VSMC) as model mammalian cells.

To this end, VSMC are trapped in the incubation chamber, where they proliferate under optimal experimental conditions (37 °C, 5% CO_2 and a low continuous flow of Dulbecco's Modified Eagle Medium (DMEM) at 0.5 μL min^{-1} to avoid shear stress). During proliferation, cell metabolism transforms big substrates in small molecules such as CO_2 that acidify the culture medium. pH can be monitored by following the change of color of pH indicator phenol red already present in the culture medium. Concretely, phenol red presents two forms absorbing at 440 nm (protonated form) and 560 nm (deprotonated form), whose magnitude varies with the pH, as shown in Figure 4d. Thus, monitoring these absorption bands it is possible to follow pH changes in the culture medium with precision. The pH is determined through the 560 nm band for presenting higher sensitivities and low interference of other absorbing components of the medium (e.g., fetal bovine serum that absorbs at 390 nm).

In this case, pH is monitored in both incubation and monitoring chambers with a 180° configuration. Results are illustrated in Figure 4e. As shown, dispersion due to the attachment/detachment of cells interferes with the pH determination in the incubation chamber. Conversely, pH changes are determined in real-time, with precision and without interferences in the monitoring chamber.

Moreover, although control and monitoring of pH is a critical issue for cell engineering, this bioPhLoC may also be used to monitor other small or large molecules assimilated or secreted by cells. One interesting application may be the analysis of proteins, carbohydrates, or DNA/RNA secreted by cells. Detection of these molecules/compounds requires very energetic UV radiation.[35] As with bioPhLoC, cell proliferation and monitoring are performed in separated chambers, and secreted molecules can be measured in the monitoring chamber with high energetic UV light sources without compromising cell viability or the biological processes taking place there. Thus, bioPhLoC may be an ideal tool for secretomics, which is the analysis of secreted proteins of a culture.

Modular Optofluidic Configuration. The previous examples demonstrate that complex analytical systems can be developed for specific applications by monolithic integration of micro-optics with the microfluidic elements. While monolithic integration has undisputable benefits, reconfiguration requires an entirely new cycle of fabrication, from design to master fabrication and soft-lithography. Alternatively, a modular

DOI: 10.1021/acs.analchem.6b00377
Anal. Chem. 2016, 88, 6630−6637

approach can be pursued by separately fabricating functional units and achieve more flexibility for the user, postponing the assembly to the laboratory. The major challenge in this approach is to ensure the alignment of the optical axes during the assembly.

The Modular Optofluidic System (MOPS) represented in Figure 5 consists of several interchangeable pieces with distinct functions (Figure 5a) that can be easily assembled. All modules are fabricated using two-layer soft lithographic technology and each one exhibits plugs and sockets for reciprocal anchorage, thus ensuring optimal alignment and tight interconnections. Fluidic modules are plasma-bonded before use. The latter step, in combination with an air bubble based internal pressure regulator at the fluidic inlet (Figure 5a-3), allows obtaining a configurable-on-demand and completely leak-free microfluidic structure. The micro-optic modules are subsequently reversibly attached to the microfluidic structure and can be reconfigured according to the application. The system has been validated in proof-of-concept experiments for absorbance measurements in a 180° configuration using crystal violet as target analyte (as depicted in Figure 5a) and, as shown in Figure 5b,c, in a reconfigured 90° fluorescence configuration using fluorescein as target analyte. Here, excitation and detection axes are perpendicular to avoid background noise from nonabsorbed excitation radiation. An additional sol–gel absorbance filter[34] (module 2 in Figure 5a) blocks stray excitation radiation, further improving the SNR.

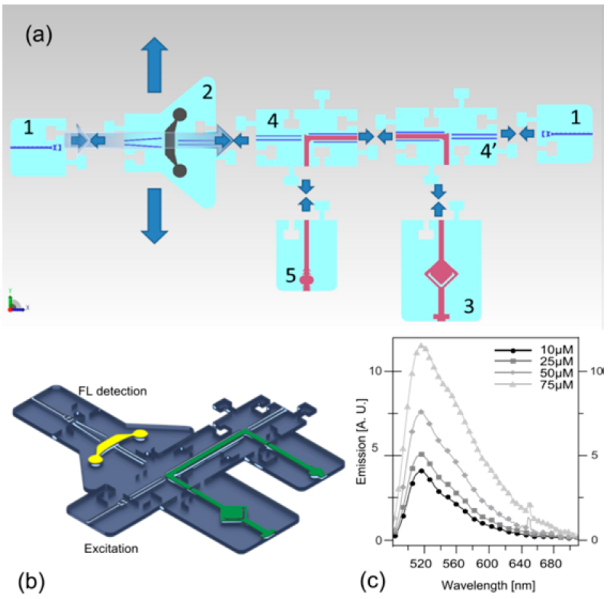

Figure 5. (a) Design-scheme of the MOPS used in this work. The individual modules are (1) two fiber optics connections, (2) a solid/liquid absorbance filter (filled with a colorant or a doped sol–gel) which can be included or excluded as required, (3) a fluidic inlet port with an internal air bubble based pressure regulator, (4/4′) two waveguides directed to a microchannel which is shielded with air mirrors to prevent optical cross-talk, (5) a fluidic outlet port. (b) 90° Configuration for fluorescence measurements; (c) emission spectra of aqueous fluorescein solutions with different concentrations. Figures published in ref 36 and reproduced by permission of The Royal Society of Chemistry. Copyright 2014.

CONCLUSIONS

In this work we present fundamentals behind the design and operation of PhLoC based on the low-cost integration of three of the most widespread standard spectrophotometric analytical techniques: colorimetry in the UV–vis range, fluorimetry, and dispersion/scattering measurements. The fabrication of monolithically integrated micro-optic elements and its design only considering well-defined interphase surfaces and the refractive index variation among construction materials, surrounding air and analyte solutions has been explained and depicted through different PhLoC approaches dealing with common analytical problems. The use of micro-optic elements for light beam collimation has been presented, demonstrating to be extremely valuable for the boosting of light–sample interaction in optofluidic systems and therefore for the increase of the analytical sensitivity.

ASSOCIATED CONTENT

Supporting Information

The Supporting Information is available free of charge on the ACS Publications website at DOI: 10.1021/acs.analchem.6b00377.

Ready-to-use CAD design of microlenses and self-alignment channel for PDMS and pig-tailed fiber optics with NA = 0.22 (PDF)

AUTHOR INFORMATION

Corresponding Author

*E-mail: Andreu.llobera@imb-cnm.csic.es.

Author Contributions

§I.R.-R. and T.N.A. equally contributed to this work. Both should be considered as first authors. The manuscript was written through contributions of all authors. All authors have given approval to the final version of the manuscript.

Notes

The authors declare no competing financial interest.

Biographies

Isaac Rodríguez-Ruiz has a Ph.D. in Chemistry (2013). He is currently a research fellow at the Laboratoire de Génie Chimique et Instrumentation (LGCI) at the French Alternative Energies and Atomic Energy Commission (DTEC/CEA-Marcoule). The main objects of his research are the development of novel analytical tools and photonic lab-on-a-chip platforms for precipitation studies related to hydrometallurgical processes and nuclear waste treatment.

Tobias N. Ackermann is currently a Ph.D. student at the Institut de Microelectrònica of Barcelona (CSIC). His studies are centered in the implementation of biological samples as photonic structures in photonic lab-on-a-chip platforms.

Xavier Muñoz-Berbel earned a Ph.D. in biotechnology (2008) and is a tenure-track researcher at the Institut de Microeletrònica de Barcelona (CSIC). His current research combines methodological, technological, and instrumental advances for biological science applications.

Andreu Llobera received a Ph.D. in Physics in 2002. Since 2009, he has held a permanent position as a researcher at the CSIC. He has coauthored more than 100 published articles. His research activities include integrated optics devices and photonic lab-on-a-chip platforms, either using silicon or polymer technology. Dr. Llobera was awarded a Starting Grant of the European Research Council in 2008.

DOI: 10.1021/acs.analchem.6b00377
Anal. Chem. 2016, 88, 6630–6637

■ ACKNOWLEDGMENTS

This work has been partly funded by the European Commission (Contract No. 317916) under the LiPhos project. I.R. thanks the CEA-Enhanced Eurotalents Program for his Incoming CEA postdoctoral fellowship. X.M.B. acknowledges the MINECO for the award of a Ramón y Cajal contract.

■ REFERENCES

(1) Manz, A.; Graber, N.; Widmer, H. á. *Sens. Actuators, B* **1990**, *1* (1), 244−248.
(2) (a) Wu, M.-H.; Huang, S.-B.; Lee, G.-B. *Lab Chip* **2010**, *10* (8), 939−956. (b) Rodríguez-Ruiz, I.; Llobera, A.; Vila-Planas, J.; Johnson, D. W.; Gómez-Morales, J.; García-Ruiz, J. M. *Anal. Chem.* **2013**, *85* (20), 9678−9685.
(3) Marcus, J. S.; Anderson, W. F.; Quake, S. R. *Anal. Chem.* **2006**, *78* (3), 956−958.
(4) Martinez, A. W.; Phillips, S. T.; Whitesides, G. M.; Carrilho, E. *Anal. Chem.* **2010**, *82* (1), 3−10.
(5) Shevkoplyas, S. S.; Yoshida, T.; Munn, L. L.; Bitensky, M. W. *Anal. Chem.* **2005**, *77* (3), 933−937.
(6) Kimmel, D. W.; LeBlanc, G.; Meschievitz, M. E.; Cliffel, D. E. *Anal. Chem.* **2012**, *84* (2), 685−707.
(7) Hoshino, K.; Huang, Y.-Y.; Lane, N.; Huebschman, M.; Uhr, J. W.; Frenkel, E. P.; Zhang, X. *Lab Chip* **2011**, *11* (20), 3449−3457.
(8) Balslev, S.; Jorgensen, A.; Bilenberg, B.; Mogensen, K. B.; Snakenborg, D.; Geschke, O.; Kutter, J. P.; Kristensen, A. *Lab Chip* **2006**, *6* (2), 213−217.
(9) Lepage, D.; Jiménez, A.; Beauvais, J.; Dubowski, J. J. *Light: Sci. Appl.* **2013**, *2* (4), e62.
(10) (a) Psaltis, D.; Quake, S. R.; Yang, C. *Nature* **2006**, *442* (7101), 381−386. (b) Monat, C.; Domachuk, P.; Eggleton, B. *Nat. Photonics* **2007**, *1* (2), 106−114.
(11) Llobera, A.; Demming, S.; Wilke, R.; Büttgenbach, S. *Lab Chip* **2007**, *7* (11), 1560−1566.
(12) Mayers, B. T.; Vezenov, D. V.; Vullev, V. I.; Whitesides, G. M. *Anal. Chem.* **2005**, *77* (5), 1310−1316.
(13) Müller, P.; Kopp, D.; Llobera, A.; Zappe, H. *Lab Chip* **2014**, *14* (4), 737−743.
(14) Swinehart, D. F. *J. Chem. Educ.* **1962**, *39* (7), 333.
(15) Valeur, B. *Molecular Fluorescence: Principles and Applications*; Wiley-VCH Verlag GmbH: Weinheim, Germany, 2001; Vol. *8*.
(16) Kwan, A.; Dudley, J.; Lantz, E. *Phys. World* **2002**, *15* (4), 64.
(17) Vila-Planas, J.; Fernández-Rosas, E.; Ibarlucea, B.; Demming, S.; Nogués, C.; Plaza, J. A.; Domínguez, C.; Büttgenbach, S.; Llobera, A. *Nat. Protoc.* **2011**, *6* (10), 1642−1655.
(18) Llobera, A.; Wilke, R.; Büttgenbach, S. *Talanta* **2008**, *75* (2), 473−479.
(19) Llobera, A.; Wilke, R.; Büttgenbach, S. *Lab Chip* **2004**, *4* (1), 24−27.
(20) Llobera, A.; Wilke, R.; Büttgenbach, S. *Lab Chip* **2005**, *5* (5), 506−511.
(21) Ibarlucea, B.; Díez-Gil, C.; Ratera, I.; Veciana, J.; Caballero, A.; Zapata, F.; Tárraga, A.; Molina, P.; Demming, S.; Büttgenbach, S. *Analyst* **2013**, *138* (3), 839−844.
(22) Gutiérrez, M.; Llobera, A.; Vila-Planas, J.; Capdevila, F.; Demming, S.; Büttgenbach, S.; Mínguez, S.; Jiménez-Jorquera, C. *Analyst* **2010**, *135* (7), 1718−1725.
(23) Ibarlucea, B.; Fernández-Sánchez, C.; Demming, S.; Büttgenbach, S.; Llobera, A. *Analyst* **2011**, *136* (17), 3496−3502.
(24) Long, G. L.; Winefordner, J. D. *Anal. Chem.* **1983**, *55* (7), 712A−724A.
(25) Ordeig, O.; Ortiz, P.; Muñoz-Berbel, X.; Demming, S.; Büttgenbach, S.; Fernández-Sánchez, C. s.; Llobera, A. *Anal. Chem.* **2012**, *84* (8), 3546−3553.
(26) Gutiérrez-Capitán, M.; Santiago, J.-L.; Vila-Planas, J.; Llobera, A.; Boso, S.; Gago, P.; Martínez, M.-C.; Jiménez-Jorquera, C. *J. Agric. Food Chem.* **2013**, *61* (39), 9325−9332.
(27) Ibarlucea, B.; Fernandez-Rosas, E.; Vila-Planas, J.; Demming, S.; Nogues, C.; Plaza, J. A.; Büttgenbach, S.; Llobera, A. *Anal. Chem.* **2010**, *82* (10), 4246−4251.
(28) Llobera, A.; Juvert, J.; González-Fernández, A.; Ibarlucea, B.; Carregal-Romero, E.; Büttgenbach, S.; Fernández-Sánchez, C. *Light: Sci. Appl.* **2015**, *4* (4), e271.
(29) Rodríguez-Ruiz, I.; Conejero-Muriel, M.; Ackermann, T. N.; Gavira, J. A.; Llobera, A. *Lab Chip* **2015**, *15* (4), 1133−1139.
(30) El-Ali, J.; Sorger, P. K.; Jensen, K. F. *Nature* **2006**, *442* (7101), 403−411.
(31) Meyvantsson, I.; Beebe, D. J. *Annu. Rev. Anal. Chem.* **2008**, *1*, 423−449.
(32) Voldman, J.; Gray, M. L.; Schmidt, M. A. *Annu. Rev. Biomed. Eng.* **1999**, *1* (1), 401−425.
(33) Muñoz-Berbel, X.; Rodríguez-Rodríguez, R.; Vigués, N.; Demming, S.; Mas, J.; Büttgenbach, S.; Verpoorte, E.; Ortiz, P.; Llobera, A. *Lab Chip* **2013**, *13* (21), 4239−4247.
(34) Carregal-Romero, E.; Fernández-Sánchez, C.; Eguizabal, A.; Demming, S.; Büttgenbach, S.; Llobera, A. *Opt. Express* **2012**, *20* (21), 23700−23719.
(35) (a) Vorndran, A.; Oefner, P.; Scherz, H.; Bonn, G. *Chromatographia* **1992**, *33* (3−4), 163−168. (b) Barbas, C. F.; Burton, D. R.; Scott, J. K.; Silverman, G. J. *Cold Spring Harbor Protocols* **2007**, *2007* (11), pdb.ip47.
(36) Ackermann, T. N.; Álvarez-Conde, E.; Vila-Planas, J.; Müller, P.; Lorenz, T.; Dietzel, A.; Zappe, H.; Muñoz-Berbel, X.; LLobera, A. Modular optofluidic systems. In *microTAS 2014*, San Antonio, TX, 2014.

DOI: 10.1021/acs.analchem.6b00377
Anal. Chem. 2016, 88, 6630−6637